Available online at www.sciencedirect.com
SCIENCE DIRECT®
Journal of Power Sources 146 (2005) 501–506
JOURNAL OF POWER SOURCES
www.elsevier.com/locate/jpowsour

TiO_2–B nanowires as negative electrodes for rechargeable lithium batteries

A. Robert Armstrong, Graham Armstrong, Jesus Canales, Peter G. Bruce *

School of Chemistry, University of St. Andrews, Purdie Building, St Andrews KY16 9ST, UK

Available online 26 April 2005

Abstract

TiO_2–B nanowires (20–40 nm diameter) may be prepared in high yield by a simple synthetic procedure. Lithium may be intercalated up to $Li_{0.91}TiO_2$–B corresponding to a capacity of 305 mAh g^{-1} and at a potential of 1.6 V versus Li^+ (1 M)/Li. This can be compared with 160 mAh g^{-1} for $Li_4Ti_5O_{12}$ and 165 mAh g^{-1} for TiO_2-anatase. Following a small irreversible capacity on the first cycle, capacity retention is excellent corresponding to a fade of <0.1% per cycle at a rate of 50 mA g^{-1}. A capacity of 160 mAh g^{-1} is sustained at a rate of 500 mA g^{-1} in electrodes that were not optimised for rate capability. Results to date indicate that the small irreversible loss of capacity on the first cycle is not associated with a SEI layer.
© 2005 Elsevier B.V. All rights reserved.

Keywords: TiO_2–B nanowires; TiO_2-anatase; Negative electrode

1. Introduction

The carbon negative electrode used in rechargeable lithium-ion cells (C/electrolyte/$LiCoO_2$) suffers from a number of problems; most notably the potential for lithium intercalation is close to that of the Li^+/Li redox couple, leading to the possibility of lithium plating during charge and hence significant safety concerns, also charge must be consumed in order to form the SEI layer (essential to the operation of the carbon electrode) on the first charge cycle. These issues are coming increasingly into focus because of the efforts to develop larger cells that are capable of sustaining higher charge–discharge rates, for applications such as hybrid electric vehicles and renewable energy storage. As a result, there is now great interest in alternative anodes which operate at higher voltages, especially the titanate spinel $Li_{4+x}Ti_5O_{12}$, $0 < x < 3$, the potential of which is ~1.5 V versus Li^+ (1M)/Li [1–6]. Use of such an anode reduces the overall cell voltage but it is reported to provide cells with enhanced safety, good capacity retention on cycling and low self-discharge. Such titanates are also of interest as anodes in hybrid supercapacitors, where they are combined with a carbon positive electrode and a non-aqueous electrolyte [7–9]. Other titanates, including anatase, have also been studied as electrodes [10–12].

Nanotubes/wires based on oxides, especially TiO_2, are of considerable interest because their dimensional confinement can enhance some of the properties associated with these materials. Recently, it has been shown that early work on the synthesis of TiO_2 nanotubes/wires resulted, not in the formation of TiO_2, but instead of nanotubes/wires composed of the sodium hydrogen titanate $Na_{2-x}H_xTi_nO_{2n+1}$ [13–17]. We have synthesised and characterised the first example of TiO_2 nanowires but with the TiO_2–B structure [18,19]. This polymorph of TiO_2 is composed of edge and corner sharing TiO_2 octahedra which form an open framework structure that is less dense than rutile, anatase or brookite and is capable of acting as an intercalation host for Li [20–22]. Exploiting the properties of nanotubes is often hampered by the fact that their synthesis can be difficult, costly, provide only small quantities and in small yield, and may be difficult to scale up. This is particularly true for application in power sources. In contrast, the synthesis of TiO_2–B nanowires is simple, requiring only NaOH, TiO_2-anatase and water, can provide relatively large quantities of material and in high yield. Given these facts and

* Corresponding author. Tel.: +44 1334 463825; fax: +44 1334 463808.
E-mail address: pgb1@st-and.ac.uk (P.G. Bruce).

0378-7753/$ – see front matter © 2005 Elsevier B.V. All rights reserved.
doi:10.1016/j.jpowsour.2005.03.057

the intense current interest in titanate anodes, it is useful to consider further the properties of TiO_2–B nanowires as possible negative electrodes in electrochemical energy storage devices such as rechargeable lithium batteries.

2. Experimental

Titanate nanowires were synthesized by adding 6 g of anatase TiO_2 to a 15 M aqueous solution of NaOH. After stirring for 1 h, the resulting suspension was transferred to a Teflon-lined autoclave and heated to 170 °C for 72 h. The product was acid-washed, which involved stirring the sample in 0.05 M HCl solution for 2 h. The material was then filtered, washed with distilled water and dried at 80 °C for 15 h. TiO_2–B nanowires were prepared by heating the acid-washed titanate nanowires at 400 °C for 4 h in air. Room temperature powder X-ray diffraction was performed on a Stoe STADI/P diffractometer operating in transmission mode with Cu $K\alpha_1$ radiation. Transmission electron microscopy was performed on a Jeol JEM-2011 instrument fitted with an EDX facility. Electrochemical properties were measured on electrodes prepared using mixtures comprising 75% active material, 18% Super S carbon and 7% PTFE, pressed into pellets. In order to investigate rate capability, three-electrode cells were employed since on cycling two-electrode cells at high rate significant overpotential related to plating and stripping of lithium at the Li electrode can affect the results. For these cells, 75% active material, 18% Super S carbon and 7% Kynar Flex 2801 (a copolymer based on PVDF) was prepared as a slurry in THF and spread onto aluminium foil using a Doctor Blade technique. The cells consisted of this electrode, lithium metal counter/reference electrodes and the electrolyte, a 1m solution of $LiPF_6$ in ethylene carbonate/dimethyl carbonate 1:1 (v/v (Merck)). All cells were constructed and handled in an Ar filled MBraun glovebox. Electrochemical measurements were carried out at 30 °C using a Biologic MacPile II system.

AC impedance data were collected using a Solartron 1255 Frequency Response Analyser connected to a Solartron 1286 Electrochemical Interface (potentiostat). A perturbation of 10 mV was applied and data collected under PC control (custom software) from 200 kHz to 10 mHz.

3. Results and discussion

A powder X-ray diffraction pattern for TiO_2–B nanowires is compared with that for bulk TiO_2–B in Fig. 1; these data demonstrate that the nanowires adopt the TiO_2–B structure, although with broadened peaks. The low resolution TEM of the as-prepared nanowires is shown in Fig. 1(b) and confirms the morphology and high yield of nanowires. The TiO_2–B nanowires are of typical diameter 20–40 nm and can extend up to several micrometers in length. Sample sizes of several grams may readily be obtained in the laboratory.

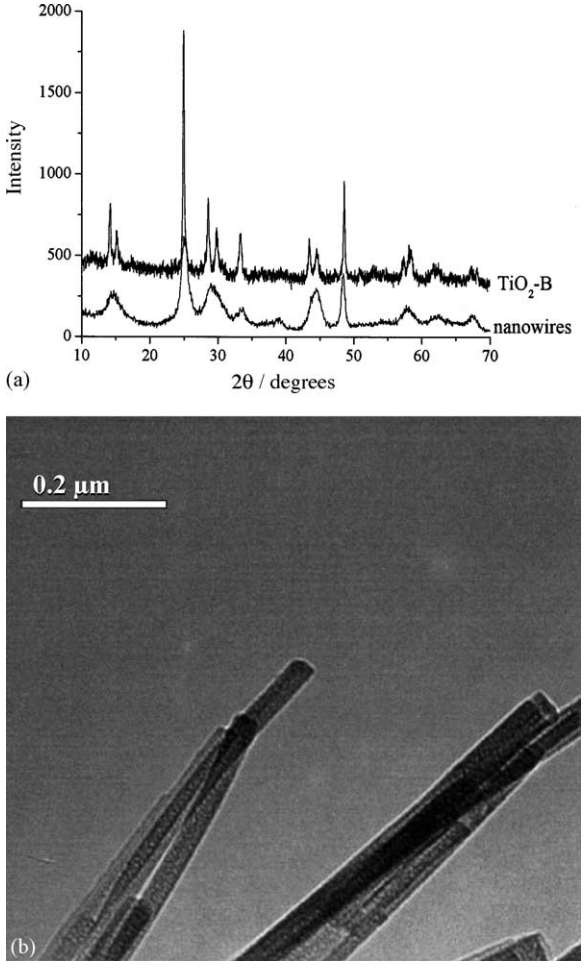

Fig. 1. (a) Powder X-ray diffraction pattern for TiO_2–B nanowires prepared by heating at 400 °C for 4 h in air. A powder pattern for TiO_2–B is shown for comparison. (b) Low resolution TEM image of the TiO_2–B nanowires.

A plot of the variation of potential as a function of lithium content during the first discharge (Li intercalation), then charge (Li deintercalation) and at a low rate of 10 mA g^{-1} is shown in Fig. 2(a), the associated differential capacity plot, dQ/dE, is presented in Fig. 2(b). Data for bulk TiO_2–B, collected under identical conditions, are also presented in Fig. 2 for comparison. As expected for the $Ti^{4+/3+}$ couple in an octahedral oxygen environment, the potential is ∼1.6 V versus Li^+ (1 M)/Li and exhibits relatively little difference between the charge and discharge plots. The discharge capacity is 305 mAh g^{-1}, which corresponds to a composition $Li_{0.91}TiO_2$–B. A small irreversible capacity (charge capacity less than discharge) of 25 mAh g^{-1}. It should be noted that the first cycle charge–discharge curve for TiO_2–B nanowires, collected under identical conditions to those used here, has been reported previously (see inset) [18]. The two curves are very similar except that previously the maximum capacity on discharge was slightly lower at 275 mAh g^{-1} corresponding to $Li_{0.82}TiO_2$–B and the irreversible capacity was 50 mAh g^{-1} twice the value for the data reported in Fig. 2(a). This variation may be due to differences between batches of

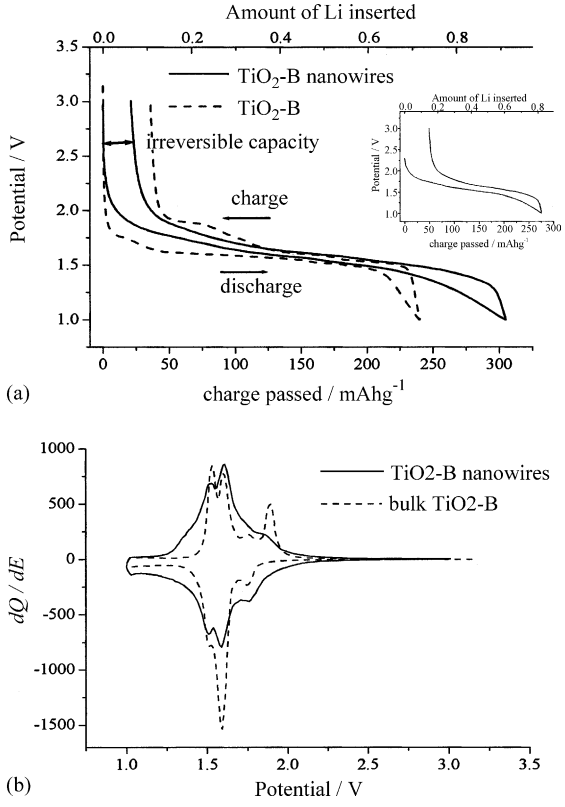

Fig. 2. (a) Variation of potential vs. Li/Li^+ (1 M) electrode, with Li content (charge passed) for TiO_2–B nanowires and normal TiO_2–B cycled under identical conditions. Rate, 10 mA g^{-1} (current of 10 mA g^{-1} of TiO_2–B) and voltage limits of 1 and 3 V. Inset shows an equivalent discharge curve for TiO_2–B nanowires illustrating variation in irreversible capacity. (b) Incremental capacity plots for TiO_2–B nanowires and normal TiO_2–B cycled at 10 mA g^{-1} between voltage limits of 1 and 3 V.

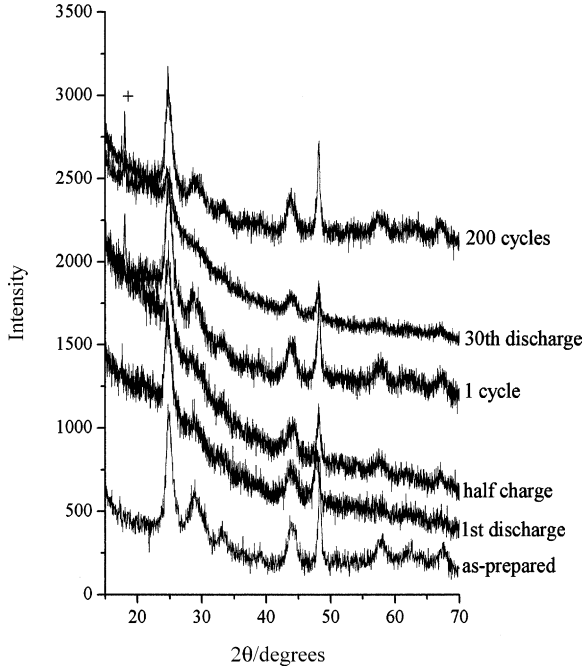

Fig. 3. Powder X-ray diffraction pattern for TiO_2–B nanowires at various states of charge and after extended cycling. '+' indicates peak from PTFE binder.

TiO_2–B nanowires but is more likely due to the poor intrinsic electronic conductivity of the material, which renders it particularly sensitive to the distribution of the super S carbon in the composite electrode. Further work is underway to explore the origin of this improvement in the later cells compared with the earlier work. The irreversible capacity loss is discussed later in this paper. The capacity to intercalate Li into TiO_2–B nanowires is greater than TiO_2-anatase ($Li_{0.5}TiO_2$, 165 mAh g^{-1}) and $Li_4Ti_5O_{12}$ ($Li_7Ti_4O_{12}$, 175 mAh g^{-1}). Generally, the latter electrode exhibits, in practice, a capacity closer to 160 mAh g^{-1} [1–6]. Comparison of the data in Fig. 2 for the nanowires and bulk TiO_2–B indicates that the dimensional confinement of the former has little effect on the potential. In particular, Fig. 2(b), which is sensitive to the presence of plateaus in the curves in (a), these appearing as peaks in (b), indicates that the energetics of Li^+ and e^- intercalation into the host is very similar for the dimensionally confined nanowires and the bulk material, consistent with the Li^+ and e^- energetics being dominated by short range forces.

Fig. 2(b) indicates that there are three pairs of peaks at 1.5, 1.6 and 1.75 V corresponding to plateaus in the load curve. A fourth oxidation peak is present at 1.9 V and is particularly prominent in the bulk TiO_2–B data. Either this oxidation is irreversible or the corresponding reduction process overlaps with one of the other reduction peaks. It is apparent that the 1.6 V reduction peak for bulk TiO_2–B is relatively larger than that at 1.5 V compared with the same peaks for the nanowires, and this larger peak at 1.6 V may be associated with the 1.9 V oxidation.

Despite several features being evident in Fig. 2(b) none of them reflect gross structural changes in the nanowires, as shown by the powder X-ray diffraction data in Fig. 3. There are no major differences in the powder X-ray diffraction patterns for cells arrested at the end of discharge (1 V) half-charge (1.55 V) or after 1, 30 and 200 cycles. The only perceptible change is a slight shift in the peaks to lower 2θ on intercalation (discharge) consistent with a slight expansion of the unit cell. The $h\,k\,l$ dependent peak broadening and lattice parameter shift is discussed in more detail elsewhere [19]. This suggests that structural changes associated with any of the features evident in Fig. 2 are more likely due to subtle effects, such as Li^+ and/or e^- ordering or multiple Li^+ sites within the TiO_2–B framework. More detailed structural studies using neutron diffraction are underway to determine the location of Li^+ in Li_xTiO_2–B as a function of x and to relate these to some or all of the features in Fig. 2(b).

The structural stability anticipates good capacity retention on cycling. A number of charge–discharge curves are presented in Fig. 4, all collected at a rate of 50 mA g^{-1}. The small irreversible capacity loss on the first cycle (Fig. 2(a)), reduces the capacity on the second cycle, however, thereafter the capacity retention is excellent with a loss of less than 0.1% per cycle from cycles 2 to 100. In fact, the fade between cycles

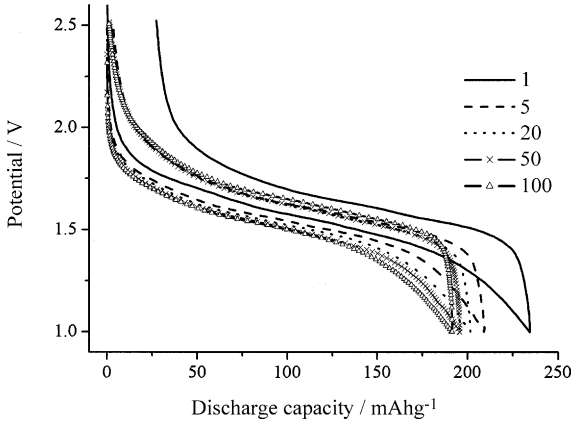

Fig. 4. Load curves for TiO_2–B nanowires at a rate of 50 mA g^{-1} between voltage limits of 1 and 2.5 V.

20 and 100 is even less at 0.06% per cycle. The shape of the load curve is also remarkably stable with cycling emphasising the excellent reversibility of intercalation/deintercalation. It is also worth noting that the charge–discharge efficiency is within error of 100%. Such stability in capacity bodes well for the use of these materials as possible electrodes in cells.

Let us return to the irreversible capacity loss observed in Figs.2(a) and 4. Such irreversible capacity on carbon is associated with SEI layer formation. However, the low voltage cut-off used here is 1 V and this should minimise electrolyte reduction and hence any SEI layer formation. Previous literature reports suggest that SEI layer formation does not occur on $Li_4Ti_5O_{12}$ electrodes if cycling is confined to potentials greater than 1 V [23,24]. Transmission electron micrographs were taken of the nanowires at the end of discharge (1 V) (Fig. 5). These show no visible evidence of SEI layer formation even at high magnification. AC impedance data were

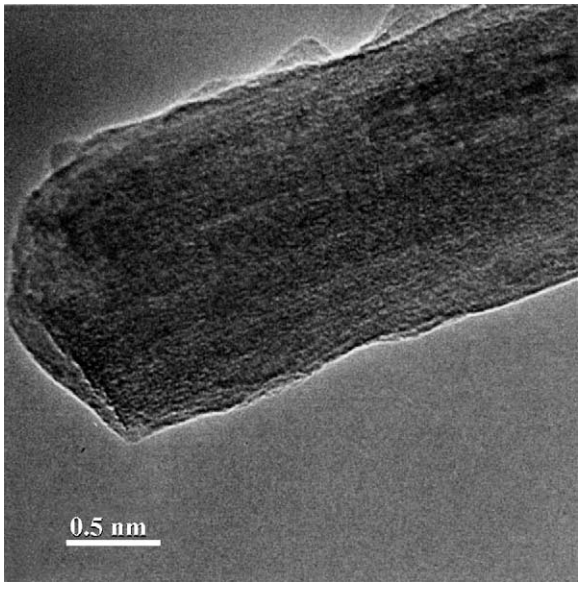

Fig. 5. High resolution TEM image of a TiO_2–B nanowire after discharging to 1 V.

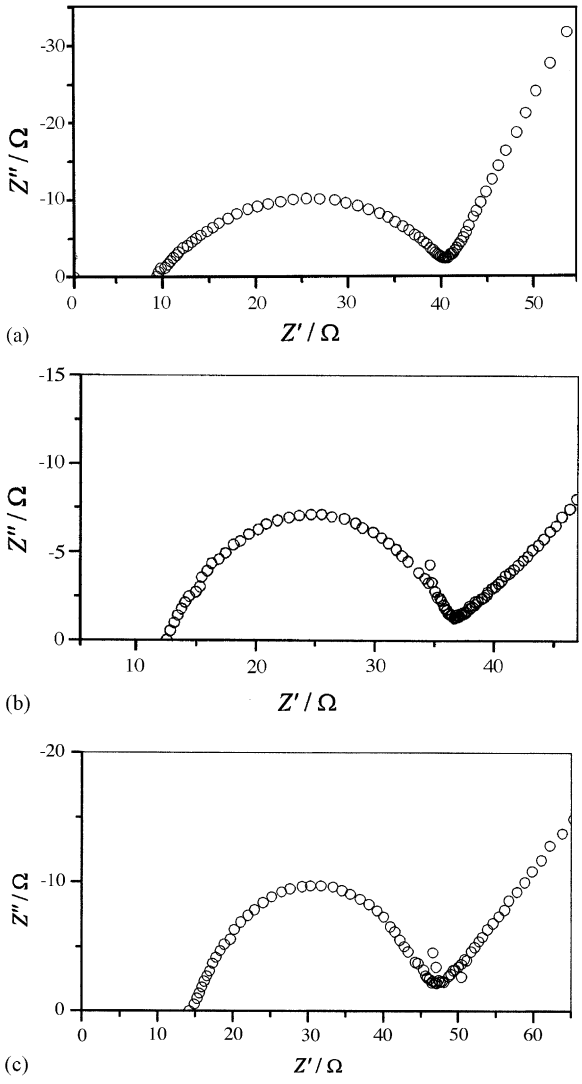

Fig. 6. AC impedance plots for TiO_2–B nanowires: (a) at open circuit, (b) after discharging to 1.55 V and (c) after discharging to 1 V.

collected on three-electrode cells so as to focus attention on the TiO_2–B nanowire (working) electrode/electrolyte interface. These data (Fig. 6) were collected at different potentials during the first discharge, then charge. The cells were arrested at the potentials noted in the figure and held at these potentials during collection of the AC data. In all cases, and crucially at 1 V, only one semicircle is evident and with a capacitance of 2.5 μF cm^{-2}, typical for an electrode/electrolyte double layer capacitance. This is consistent with the absence of a SEI layer on the TiO_2–B surface.

A number of other explanations are possible for the irreversible capacity losses. For example, it may be difficult to remove all the Li that is intercalated on the first cycle, due perhaps to a minor structural change not evident in the broad powder XRD patterns in Fig. 3. Alternatively, the poor intrinsic electronic conductivity of TiO_2–B may, on recharge, result in regions near the surface becoming depleted of $Li^+ + e^-$, with the latter resulting in poor electronic conductivity and

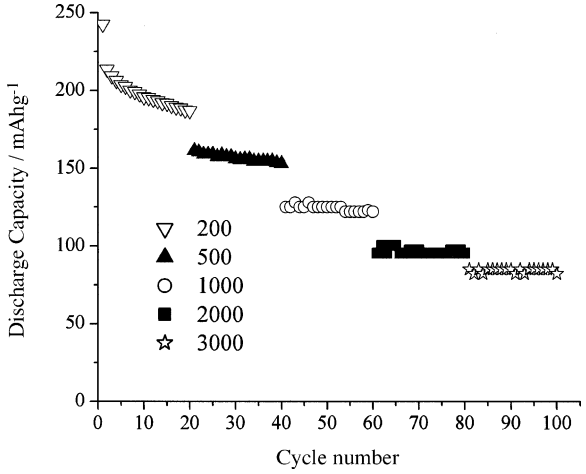

Fig. 7. Variation in discharge capacity vs. cycle number for TiO_2–B nanowires cycled at 200, 500, 1000, 2000 and 3000 mA g^{-1} between voltage limits of 1.2 and 2.5 V.

hence significant polarisation, such that the remaining Li is not easily removed. After completing one cycle at a rate of 10 mA g^{-1}, a cell was held at 3 V for 48 h, resulting in removal of 40% of the "irreversible" capacity. In case of this cell, the irreversible capacity before the potentiostatic hold was 21 mAh g^{-1} and after 13 mAh g^{-1}, the remaining irreversible capacity corresponded to only 4% of the discharge capacity for this cell. These results plus the variability in the amount of irreversible capacity noted from cell to cell (see Fig. 2(a)) suggest that it should be possible to reduce the irreversible capacity still further and to levels suitable for applications. Indeed, if the poor electronic conductivity is a problem then strategies for coating the particles with an electronic conductor, such as those used successfully for $LiFePO_4$, may be of value here. Further work is underway to determine the source of the irreversible capacity and to minimise it consistently.

One of the most interesting features of the nanowire morphology is the potential to support high charge–discharge rates. To evaluate the rate capability, three electrode cells were used. This was done to ensure that any polarisation occurring at the lithium electrode in a two-electrode cell, which might influence the measurements, was eliminated. The results of the three electrode rate measurements are reported in Fig. 7. These data indicate that the nanowires exhibit significant capacity at high rates; for example, a capacity of 160 mAh g^{-1} at a rate of 500 mA g^{-1} (corresponding to a practical *C* rate of 3*C*) was obtained and a discharge capacity of 100 mAh g^{-1} at 2000 mA g^{-1} (20*C*) was observed. These results were collected on electrodes cast with Kynar as binder rather than pressed into disks with PTFE. The former construction is less rate limiting, as demonstrated by the fact that that the same capacity was observed at 200 mA g^{-1} for the cast electrode as was obtained from the disk electrode at 50 mA g^{-1}. Nevertheless, the cast electrodes are not optimised and the poor intrinsic conductivity of TiO_2–B, discussed above, may be rate limiting so that improved composite electrodes and/or coated particles could lead to improvements in rate capability. The results reported here do however serve to demonstrate that the TiO_2–B nanowires can deliver significant capacities at relatively high rates.

4. Conclusions

TiO_2–B nanowires may be synthesised in high yield and quantity by a simple method. Lithium may be intercalated and discharge (intercalation) capacities of 305 mAh g^{-1}, corresponding to a composition $Li_{0.91}TiO_2$–B may be obtained which is higher than the capacity for $Li_4Ti_5O_{12}$ (160 mAh g^{-1}) or TiO_2-anatase (165 mAh g^{-1}). This capacity is delivered at a potential of around 1.6 V versus Li^+ (1 M)/Li and the potential is relatively flat over most of the range. Cycling efficiency is excellent, as is the capacity retention on cycling after a small irreversible capacity on the first cycle. Although more detailed investigation of the origin of this small capacity loss is required, initial indications are that this is not due to SEI layer formation, a result that is consistent with the current view of the $Li_4Ti_5O_{12}$ electrode when cycled within a potential range above 1 V.

Acknowledgements

PGB is indebted to the EPSRC, the Royal Society and the European Union for financial support.

References

[1] E. Ferg, R.J. Gummow, A. De Kock, M.M. Thackeray, J. Electrochem. Soc. 141 (1994) 147.
[2] K. Zaghib, M. Simoneau, M. Armand, M. Gauthier, J. Power Sources 81 (1999) 300.
[3] T. Ohzuku, A. Ueda, N. Yamamoto, J. Electrochem. Soc. 142 (1995) 1431.
[4] A. Guerfi, S. Sévigny, M. Lagacé, P. Hovington, K. Kinoshita, K. Zaghib, J. Power Sources 119–121 (2003) 88.
[5] M. Kalbac, M. Zukalova, L. Kavan, J. Solid State Electrochem. 8 (2003) 2.
[6] K. Nakahara, R. Nakajima, T. Matsushima, H. Majima, J. Power Sources 117 (2003) 131.
[7] G.G. Amatucci, F. Badway, A. Du Pasquier, T. Zheng, J. Electrochem. Soc. 148 (2001) A930.
[8] A. Du Pasquier, I. Plitz, S. Menocal, G. Amatucci, J. Power Sources 115 (2003) 171.
[9] L. Kavan, M. Kalbac, M. Zukalova, I. Exnar, V. Lorenzen, R. Nesper, M. Graetzel, Chem. Mater. 16 (2004) 477.
[10] T. Ohzuku, T. Kodama, T. Hirai, J. Power Sources 14 (1985) 153.
[11] R.K.B. Gover, J.R. Tolchard, H. Tukamoto, T. Murai, J.T.S. Irvine, J. Electrochem. Soc. 146 (1999) 4348.
[12] A. Kuhn, R. Amandi, F. Garcia-Alvarado, J. Power Sources 92 (2001) 221.
[13] T. Kasuga, M. Hiramatsu, A. Hoson, Langmuir 14 (1998) 3160.
[14] G.H. Du, Q. Chen, R.C. Che, Z.Y. Yuan, L.M. Peng, Appl. Phys. Lett. 22 (2001) 3702.
[15] Q. Chen, W. Zhou, G. Du, L.-M. Peng, Adv. Mater. 14 (2002) 1208.
[16] X. Sun, Y. Li, Chem. Eur. J. 9 (2003) 2229.

[17] J. Yang, Z. Jin, X. Wang, W. Li, J. Zhang, S. Zhang, X. Guo, Z. Zhang, J. Chem. Soc. Dalton Trans. 2003 (2003) 3898.
[18] A.R. Armstrong, G. Armstrong, J. Canales, P.G. Bruce, Angew. Chem. Int. Ed. 43 (2004) 2286.
[19] A.R. Armstrong, G. Armstrong, J. Canales, R. García, P.G. Bruce, Adv. Mater. 17 (2005) 862.
[20] R. Marchand, L. Brohan, M. Tournoux, Mat. Res. Bull. 15 (1980) 1129.
[21] M. Touraoux, R. Marchand, L. Brohan, Prog. Solid State Chem. 17 (1986) 33.
[22] T.P. Feist, P.K. Davies, J. Solid State Chem. 101 (1992) 275.
[23] P.P. Prosini, R. Mancini, L. Petrucci, V. Contini, P. Villano, Solid State Ionics 144 (2001) 185.
[24] D. Peramunage, K.M. Abraham, J. Electrochem. Soc. 145 (1998) 2609.